Separated flow prediction and assessment using LES and machine learning

Cite as: AIP Conference Proceedings **2293**, 420093 (2020); https://doi.org/10.1063/5.0027925
Published Online: 25 November 2020

James C. Tyacke, and Ashley Scillitoe

Separated Flow Prediction and Assessment using LES and Machine Learning

James C. Tyacke[1,a)] and Ashley Scillitoe[2,b)]

[1]*Brunel University London, London, UK*
[2]*The Alan Turing Institute, London, UK*

[a)] james.tyacke@brunel.ac.uk
[b)]ascillitoe@turing.ac.uk

Abstract. Large Eddy Simulation is a predictive technology that has the potential to revolutionise CFD. Significant effort is now being put into improving lower order models based on high fidelity data. The current work contrasts LES and RANS for a low Reynolds number ribbed channel flow relevant to turbine and electronics cooling. The anisotropy of turbulence is chosen as a starting point to compare RANS modelling deficiencies, and it is found that there are significant differences between the anisotropy predicted by RANS and LES. In the LES, a spreading shear layer introduces anisotropic content into the passage. Downstream of the rib, scouring eddies shed from the rib destroy the classical boundary layer flow. A machine learning classifier trained on a database of similar flows is used to predict the anisotropy in the ribbed passage. The classifier is shown to be capable of predicting many of the flow features identified in the LES, demonstrating the potential of such approaches for application to this category of flows.

INTRODUCTION

Flow over bluff geometrical features is common in many areas including electronics cooling [1, 2], turbine internal and external cooling [3, 4, 5, 6], and urban environments [7, 8]. Such features often include cuboids and ribs and lead to separated flow. These flows generally also feature strong streamline curvature, high levels of anisotropy, non-local effects, stagnation, recirculation and free shear layers, where typically used Reynolds-Averaged Navier-Stokes (RANS) modelling, particularly eddy viscosity models are known to be challenged. However, the lower cost of Reynolds-Averaged Navier-Stokes (RANS) modelling drives continued use by industry. Significant effort is now being put into improving lower order models based on high fidelity data. Large Eddy Simulation is now an accessible predictive technique for low Reynolds number flows such as those found in electronics and some turbomachinery flows. Here we choose a ribbed passage flow relevant to those representing electronics chips, cable bundles or turbine internal cooling ribs in order to investigate deficiencies in RANS modelling when compared to LES. We use turbulence anisotropy as a starting point for continued research. Turbulent anisotropy is effective in transporting momentum and considered a crucial modelling aspect for mixing flows that may involve heat transfer or scalar transport.

Machine learning tools trained on high fidelity LES and direct numerical simulation (DNS) data are increasingly being used to inform and/or augment RANS modelling. For example, see the RANS trust region prediction methods proposed by Ling and Templeton [9]. In the present paper a similar classification method is applied to the ribbed channel flow, to determine whether such machine learning approaches are suitable for flow configurations such as the ribbed channel.

RIBBED CHANNEL SETUP

Figure 1 shows the ribbed channel test case. All walls are no-slip and impermeable. The domain is periodic in the axial (x) and spanwise (z) directions. An incompressible solver utilising second order central differencing spatially and Crank-Nicolson time stepping is used. A pressure gradient is imposed to fix the bulk velocity (mass flow rate). A

International Conference of Numerical Analysis and Applied Mathematics ICNAAM 2019
AIP Conf. Proc. 2293, 420093-1–420093-4; https://doi.org/10.1063/5.0027925
Published by AIP Publishing. 978-0-7354-4025-8/$30.00

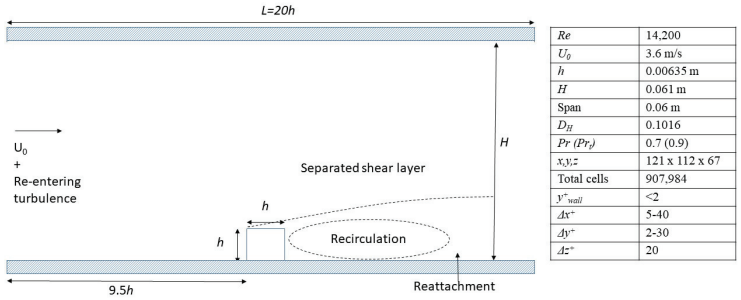

Re	14,200
U_0	3.6 m/s
h	0.00635 m
H	0.061 m
Span	0.06 m
D_H	0.1016
Pr (Pr_t)	0.7 (0.9)
x,y,z	121 x 112 x 67
Total cells	907,984
y^+_{wall}	<2
Δx^+	5-40
Δy^+	2-30
Δz^+	20

FIGURE 1. Case setup

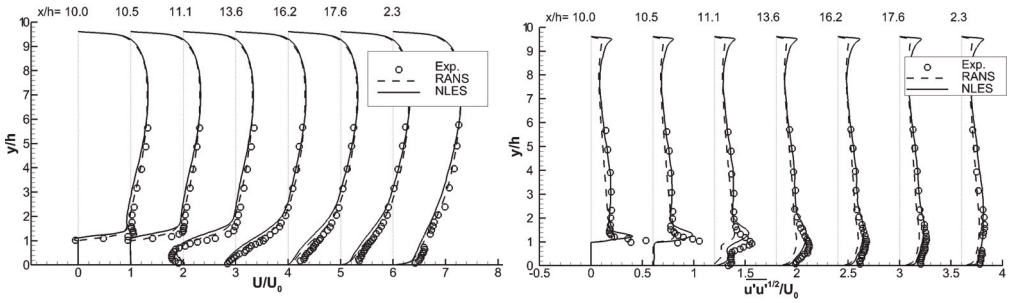

(a) (b)

FIGURE 2. (a) Mean axial velocity profiles, (b) mean axial velocity fluctuation profiles.

Numerical LES (NLES) is performed where no explicit subgrid scale model is used to avoid introducing turbulence modelling errors although some degree of modelling error arises from discretisation, however the grids used have been successfully applied in the past [1]. Flow and mesh details are provided in Figure 1. The friction Reynolds number based on the upper boundary layer is $Re_\tau = 360$. $L_x/\Delta x_{max} = 10$, where L_x is the axial integral length scale at $x - 2h, y = 0.8h$ [10]. The NLES is time-averaged for over 1000 T_h ($T_h = U_0/h$) with $CFL < 1$ and data is also span-averaged. The companion RANS was run on the same grid using the Launder-Sharma $k-\varepsilon$ model [11]. The Yap correction [12] is used to improve lengthscale prediction in the separated and stagnation regions.

RESULTS

Ribbed channel flow

Figure 2(a) shows axial mean velocity profiles at a range of axial locations for the RANS and NLES. Both are in good agreement with measurements [13]. Axial Reynolds stress (u'_{RMS}) profiles for the NLES (Figure 2(b)) are also in agreement. The RANS under-predicts the axial Reynolds stresses in the shear layer, near reattachment and towards the channel centre and the upper wall.

Poor turbulence anisotropy prediction is a key aspect limiting common RANS models. As shown in Figure 3(a), high anisotropy indicated by $\left\langle \overline{u'u'} \right\rangle / \left\langle \overline{v'v'} \right\rangle$ for this quasi 2D flow, is observed near walls and the rib shear layer. Lower anisotropy is found near reattachment, where classical boundary layer flow is destroyed by large scouring eddies shed from the rib. The spreading shear layer introduces anisotropic turbulent content at the periodic domain inlet, interacting with flow local to the rib, hence non-local effects may be important. Figure 3(b) shows the difference between the NLES and RANS of the axial component a_{11} of the turbulent anisotropy tensor ($a_{ij} = \left\langle \overline{u'_i u'_j} \right\rangle / 2k - \delta_{ij}/3$). Clearly, the RANS under-predicts anisotropy in the regions discussed.

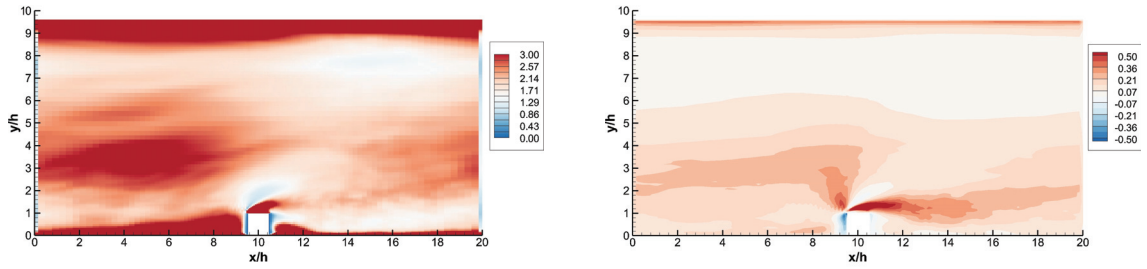

(a) (b)

FIGURE 3. Flowfield anisotropy, (a) NLES $\langle\overline{u'u'}\rangle$ / $\langle\overline{v'v'}\rangle$, (b) Δa_{11} between NLES and RANS.

Machine learning predictions

A database of canonical flow configurations for which validated DNS or LES data were available was compiled. For each DNS/LES case, shown in Table 1, a companion RANS solution was computed. The RANS solutions were converted into a matrix $\mathbf{X}$ of non-dimensional flow features. The DNS or LES datasets were converted into a binary label $y_e = (0, 1)$, where $y_e = 1$ indicates a high degree of turbulent anisotropy (based on the LES/DNS data). To quantify turbulent anisotropy the anisotropy constant $C_{aniso} = -3\lambda_3$ [14] is used, where λ_3 is the third eigenvalue of a_{ij}. The anisotropy label is set as $y_e = 1$ when $C_{aniso} > 0.5$ and $y_e = 0$ otherwise. A random forest (RF) classifier [15] is then trained on the prepared database to obtain a mapping $y_e = f_{RF}(\mathbf{X})$. The random forest model f_{RF} can predict a new anisotropy field $y_e^* = f_{RF}(\mathbf{X}^*)$ based upon a RANS feature field $\mathbf{X}^*$, which in this case is the RANS solution of the ribbed channel flow.

TABLE 1. Summary of flow cases used for training the random forest classifier.

Case	Description	Re	LES/DNS	Ref.
1	Curved backwards step	$Re_\tau = 618$	LES	[16]
2a/b/c	Convergent-divergent channel	$Re_\tau = 395/617/950$	DNS	[17], [18]
3	Periodic hills	$Re_\tau = 160$	LES	[19]
4a/b	Duct with aspect ratio $AR = 1$	$Re_\tau = 180, 360$	DNS	[20]
4c/d	Duct with aspect ratio $AR = 3$	$Re_\tau = 180, 360$	DNS	[20]

To tune the hyper-parameters of the random forest the training and validation F_1 scores are assessed using leave-one-case-out cross validation, while the number of trees in the random forest and the maximum depth of the trees are varied. Increasing both increases accuracy (plots omitted for brevity), but the gains are diminished beyond $N_{trees} = 20$. The difference between the test and training error for more complex RF models suggests a degree of over-fitting here, which could be mitigated with additional training data.

The random forest can be used to predict the probability of $y_e^* = 1$ at every point in the ribbed channel by summing the probability of each decision tree in the random forest predicting $y_e^* = 1$, based upon the provided $\mathbf{X}^*$,

$$P(y_e \mid \mathbf{X}^*) = \frac{1}{N_{trees}} \sum_{1}^{N_{trees}} P_t(y_e \mid \mathbf{X}^*). \tag{1}$$

The resulting probability field is shown in Figure 4(a). Comparing this to the "truth", which in this case is the actual C_{aniso} field in Figure 4(b), suggests that the classifier is able to predict the complex turbulent anisotropy field reasonably well. For example, the high anisotropy in the shear layer is captured, as is the region of low anisotropy where the classical boundary layer is destroyed downstream of the rib. It is important to note here that the classifier did not "see" the ribbed channel data during training, so it has been able to make this prediction based entirely upon the physics it has learned from the training flows in Table 1.

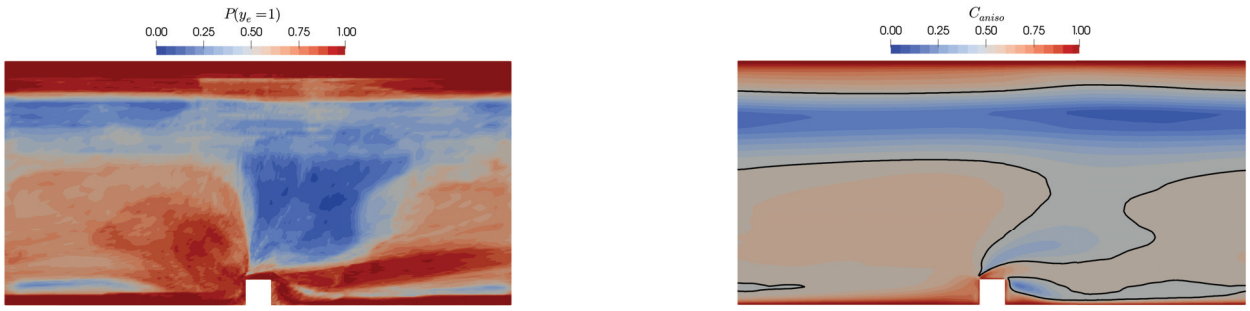

(a) (b)

FIGURE 4. Turbulent anisotropy in case 5: (a) probability of $C_{aniso} > 0.5$ predicted by RF, (b) C_{aniso} from NLES (black line is contour of $C_{aniso} = 0.5$).

CONCLUSIONS

Anisotropy is a key area where eddy viscosity models are known to be inaccurate. Significant errors between RANS and NLES Reynolds stress anisotropy were observed in a ribbed channel flow. A key area of anisotropy production is the spreading shear layer originating from the rib, while anisotropy is reduced in the shadow of the rib where large scouring eddies destroy the turbulent boundary layer. A machine learning classifier was shown to be able to predict regions of high anisotropy well, suggesting this type of flow is a suitable candidate for such techniques in the future. This offers the possibility of using ML for RANS model trust prediction, RANS-LES zonalisation and further RANS model development. The intense shear layer, vortex shedding and subsequent mixing vary spatially and temporally posing additional challenges to RANS, these will be explored in the full paper.

REFERENCES

[1] J. Tyacke and P. Tucker, Applied Mathematical Modelling **36**, 3112–3133 (2012).
[2] J. Parry, "A Complete Guide To Enclosure Thermal Design … 14 Key Considerations," Tech. Rep. (Mentor, 2017).
[3] S. Patil and D. Tafti, Journal of Turbomachinery **135**, p. 031006mar (2013).
[4] A. Rozati and D. K. Tafti, Journal of Turbomachinery **130**, p. 041015 (2008).
[5] P. Martini, a. Schulz, and H.-J. Bauer, Journal of Turbomachinery **128**, p. 196 (2006).
[6] J.-C. Han, The International Journal of Rotating Machinery **10**, 443–457nov (2004).
[7] H. Kikumoto and R. Ooka, Journal of Wind Engineering and Industrial Aerodynamics **104-106**, 516–522 (2012).
[8] D. A. Philips, R. Rossi, and G. Iaccarino, Journal of Fluid Mechanics **723**, 404–428 (2013).
[9] J. Ling and J. Templeton, Physics of Fluids **27**, p. 085103aug (2015).
[10] Y. Dai, "Large Eddy Simulation of Labyrinth Seals and Rib Shapes for Internal Cooling Passages," Phd thesis, University of Cambridge 2018.
[11] B. E. Launder and B. I. Sharma, Letters in Heat and Mass Transfer **1**, 131–138 (1974).
[12] C. J. Yap, "Turbulent Heat and Momentum Transfer in Recirculating and Impinging Flows," Phd thesis, University of Manchester 1987.
[13] S. Acharya, S. Dutta, T. A. Myrum, and R. S. Baker, International Journal of Heat and Mass Transfer **36**, 2069–2082 (1993).
[14] S. Banerjee, R. Krahl, F. Durst, and Z. Ch, Journal of Turbulence **8** (2007).
[15] L. Breiman, Machine learning **45**, 5–32 (2001), arXiv:/dx.doi.org/10.1023%2FA%3A1010933404324 [http:] .
[16] Y. Bentaleb, S. Lardeau, and M. A. Leschziner, Journal of Turbulence **13**, 1–28 (2012).
[17] M. Marquillie, J. P. Laval, and R. Dolganov, Journal of Turbulence **9**, 1–23 (2008).
[18] L. A. Schiavo, A. B. Jesus, J. L. Azevedo, and W. R. Wolf, International Journal of Heat and Fluid Flow **56**, 137–151 (2015).
[19] J. Fröhlich, C. P. Mellen, W. Rodi, L. Temmerman, and M. A. Leschziner, Journal of Fluid Mechanics **526**, 19–66 (2005).
[20] R. Vinuesa, P. Schlatter, and H. M. Nagib, Physical Review Fluids **3**, p. 054606 (2018).